Astron. Astrophys. 350, 414–422 (1999)

ASTRONOMY AND ASTROPHYSICS

On the star-formation properties of emission-line galaxies in and around voids⋆

C.C. Popescu[1,2], **U. Hopp**[3], **and M.R. Rosa**[4,⋆⋆]

[1] Max-Planck-Institut für Kernphysik, Saupfercheckweg 1, 69117 Heidelberg, Germany
[2] The Astronomical Institute of the Romanian Academy, Str. Cuţitul de Argint 5, 75212 Bucharest, Romania
[3] Universitätssternwarte München, Scheiner Strasse 1, 81679 München, Germany
[4] The Space Telescope European Coordinating Facility, European Southern Observatory, Karl-Schwarzschild-Strasse 2, 85740 Garching, Germany

Received 5 July 1999 / Accepted 26 August 1999

Abstract. We present a study of the star formation properties of a sample of emission line galaxies (ELGs) with respect to their environment. This study is part of a bigger project that aimed to find galaxies in voids and to investigate the large scale structure of the ELGs. A survey for ELGs was therefore conducted with the result that 16 galaxies have been found in very low density environments, of which 8 ELGs were found in two very well defined nearby voids. The sample presented here contains some galaxies identified in voids, as well as in the field environment that delimited the voids. These ELGs are all Blue Compact Galaxies (BCGs), and all void galaxies are also dwarfs. Both void and field sample contain the same mixture of morphological subtypes of BCDs, from the extreme Searle-Sargent galaxies to the Dwarf-Amorphous Nuclear-Starburst galaxies. The main result of this study is that field and void galaxies seem to have similar star formation rates (SFR), similar ratios between the current SFR and their average past SFR and similar mean SFR surface densities. There is no trend in metallicity, in the sense that void galaxies would have lower metallicities than their field counterparts. The field-cluster dichotomy is also discussed using available results from the literature, since our sample does not cover the cluster environment. The implication of our findings are discussed in connection with the theories for the formation and evolution of BCDs.

Key words: galaxies: abundances – galaxies: clusters: general – galaxies: compact – galaxies: dwarf – galaxies: evolution – galaxies: irregular

1. Introduction

Popescu et al. (1996, hereafter PHHE96, and 1998, hereafter PHHE98) conducted a survey for emission-line galaxies (ELGs) towards nearby voids, with the aim of finding faint galaxies within the voids. This was motivated by the question of whether the void regions represent real structures, or whether they merely appear as such due to selection effects. According to some theories of galaxy formation (Dekel & Silk 1986), that were worked out in the frame of the cold dark matter (CDM) scenarios including biasing, dwarf galaxies should originate from the $1\,\sigma$ fluctuations, and ought to be more evenly distributed than the high rare density peaks which form the giants. In these scenarios the dwarf galaxies should trace the underlying dark matter and are expected to fill the voids. Since there was a hint that emission-line galaxies are more evenly distributed (Salzer 1989, Rosenberg et al. 1994), this kind of objects were chosen to be searched, and primarily dwarf HII galaxies or BCDs. In passing we note that these two terms are used in the literature interchangeably for the same physical type of object. While the name of BCD was used for objects that were classified on morphological criteria (Binggeli et al. 1985 – for the Virgo Cluster Catalog), the term of HII galaxy was introduced for objects discovered on spectroscopic surveys for emission line galaxies (Sargent & Searle 1970, Searle & Sargent 1972).

The survey of PHHE96,PHHE98 was based on a sample selected from the Hamburg Quasar Survey (HQS) (Hagen et al. 1995) - IIIa-J digitised objective prism plates and the main selection criterion was the presence of emission-lines, mainly of the [OIII] λ5007 line. The result of the survey is that no homogeneous void population was found (Popescu et al. 1997). Nevertheless 16 ELGs were identified in very low density environments, from which at least 8 ELGs were found in two very well defined nearby voids. All the isolated galaxies were dwarf galaxies ($M_B < -18.5$, diameters $D < 10\,$kpc) of BCD class. In this paper we compare the spectroscopic properties of 11 isolated ELGs from the void environment (hereafter Void) with the spectroscopic properties of 44 galaxies from the field environment (hereafter Field), in order to evaluate the influence of the environment on the evolution of dwarf HII galaxies.

The isolated galaxies as well as those galaxies found in the filaments and sheets surrounding the voids belong to the same sample and thus they were selected with the same selection

Send offprint requests to: C.C. Popescu (popescu@levi.mpi-hd.mpg.de)

⋆ Based on observations obtained at the German-Spanish Observatory at Calar Alto, Almeria, Spain

⋆⋆ Affiliated to Astrophysics Division of the Space Science Department of the European Space Agency

criteria. Then the two subsamples do not suffer from different selection biases and therefore are valid for studies of environmental effects. Furthermore, the objects were all observed with the same telescope and set-ups, providing us with a homogeneous set of data. Popescu et al. (1997) have also shown that the sample used for the statistical analysis of the large-scale structure is a complete sample. Both subsamples contain the same type of objects, with the same morphological mixture. If, however, different subsamples containing varying percentage of morphological types are compared to infer environmental influences, then any difference found between subsamples will instead reflect the differences between different Hubble types. It could well be that this effect is the main reason behind the differing answers of different studies on environmental effects.

The influence of the environment on the mechanism that control star formation is likely one of the most important aspects in understanding the origin and evolution of galaxies. It is commonly believed that dwarf galaxies are heavily influenced by their environment. While many studies concentrated on the differences between cluster and field galaxies, very little is known about differences between Field and Void galaxies. This is especially true since voids appear to be real empty environments, while only a few galaxies were identified in these regions. Therefore the statistics of void galaxies is very poor. Much effort was put in the study of the Bootes void, a huge low density region first discovered by Kirshner et al. (1981)(see also Kirshner et al. 1983a,b). Up to now 58 galaxies were identified in this void (Szomoru et al. 1996). But Bootes void is beyond the distance at which the large scale structure is well defined by the present catalogues. Therefore it is not clear whether the galaxies found in this void are real void galaxies, or whether they are only field galaxies that were not well sampled by the present magnitude limited surveys. Weistrop et al. (1995) showed that the void galaxies in Bootes were luminous galaxies, not the low mass, low surface brightness galaxies predicted to be found in voids. We therefore especially selected nearby voids which are very well defined in the distribution of normal galaxies.

Because our sample of Void galaxies contains only 11 objects we will not try to search for statistical differences in the shape of the distributions. Thus no statistical tests (e.g. the Kolmogorov-Smirnov test) will be applied. Rather we will investigate whether the distribution of different spectroscopic parameters of Void galaxies occupies the same locus in diagrams/histograms as in the case of Field galaxies. We will show that there do not appear to be any differences between Void and Field galaxies under such a comparison.

The paper is organised as follows. In Sect. 2 we describe the sample used for the study of the environmental effects, in Sect. 3 we compare the star formation properties of Field and Void galaxies and in Sect. 4 we study the metallicities of our program galaxies with respect to their environment. In Sect. 5 we investigate the dichotomy Field - Cluster, with direct application to the galaxies in the Virgo Cluster core and in Sect. 6 we discuss our findings and we give a summary of the results.

2. The sample

In this paper we study a subsample of the ELGs found in the survey of PHHE96,PHHE98, namely galaxies in a region North to the "Slice of the Universe" (de Lapparent et al. 1986). In order to describe the large-scale structure of this region we used a comparison catalogue of giant normal galaxies, namely the ZCAT (Huchra et al. 1992, Huchra et al. 1995). The comparison catalogue should trace the main structures in the nearby Universe and should properly define the nearby voids. The region under study is dominated by the field galaxies that belong to the "Great Wall" (Ramella, Geller and Huchra 1992), at a distance of $6500\,\mathrm{km\,s^{-1}}$ at $\alpha = 12^{\mathrm{h}}00^{\mathrm{m}}$ and $9000\,\mathrm{km\,s^{-1}}$ at $\alpha = 15^{\mathrm{h}}30^{\mathrm{m}}$. At velocities less than $7500\,\mathrm{km\,s^{-1}}$, there are more field galaxies, remnants of the "Harvard Sticky Man" but without the Coma Cluster included. The field galaxies define at least two nearby voids (Popescu et al. 1997), one centred at $\alpha \sim 13^{\mathrm{h}}15^{\mathrm{m}}$, v $\sim 3000\,\mathrm{km\,s^{-1}}$, and the other one being just in front of the Great Wall. Beyond the Great Wall there is an indication of more voids, but their sizes are much less constrained by the galaxy distribution.

We restrict our analysis on ELGs with velocities less than $10000\,\mathrm{km\,s^{-1}}$, since for larger distances the comparison catalog quickly thins out, and therefore we refrain from drawing conclusions about the reality of voids beyond $10000\,\mathrm{km\,s^{-1}}$. The criteria for separating the sample in Field and Void are given in Popescu et al. (1997), based on the calculation of the nearest neighbour distances (D_{NN}). The D_{NN} represent real separations in the 3-dimensional space and are calculated (Popescu et al. 1997) as the separation between each ELG and its nearest neighbour from the comparison catalogue, for galaxies with blue magnitudes brighter than 15.5. The nearest neighbour distances of the void galaxies and their clustering properties can be found in Table 3 from Popescu et al. (1997). As an example, we illustrate the case of the void galaxy HS1236+3937 (z=0.0184). It has its nearest neighbour ZCAT galaxy at a distance $8.68\,\mathrm{h^{-1}}$ Mpc. At this redshift the average nearest neighbour distances between the field ELGs are $0.75\,\mathrm{h^{-1}}$ Mpc. Thus the galaxy HS1236+3937 differs from its field counterparts by a factor of 12 in its clustering properties. Furthermore, the mean nearest neighbour distance for the Void ELGs is $4.5\,\mathrm{h^{-1}}$ Mpc, as compared to the mean $\mathrm{D}_{NN} = 1\,\mathrm{h^{-1}}$ Mpc for the Field ELGs. The difference in the clustering properties of the two samples proves that they form two distinct populations.

The sample of ELGs, selected as described in the previous paragraph, was further constrained to contain only galaxies with reliable spectrophotometry. A list of the selected sample galaxies is given in Table 1, together with their environment: Field (F) or Void (V) galaxy (Column 9).

The spectroscopic parameters of the ELGs (emission-line ratios, equivalent widths and fluxes) together with a detailed description of the data is given by Popescu & Hopp (1999), while the photometric parameters (B and R magnitudes, diameters, morphologies and surface brightness profiles) are given by Vennik et al. (1999). In Table 1 we list only the main parameters of the selected galaxies: absolute B magnitudes (Column 2),

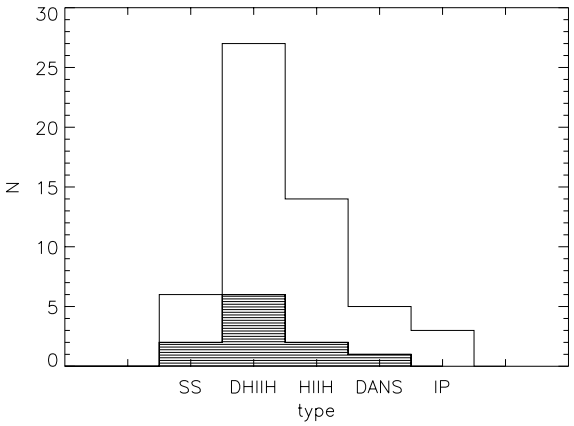

Fig. 1. The distribution of morphological types. The solid histogram is the distribution of the whole sample, while the hashed histogram is for Void galaxies.

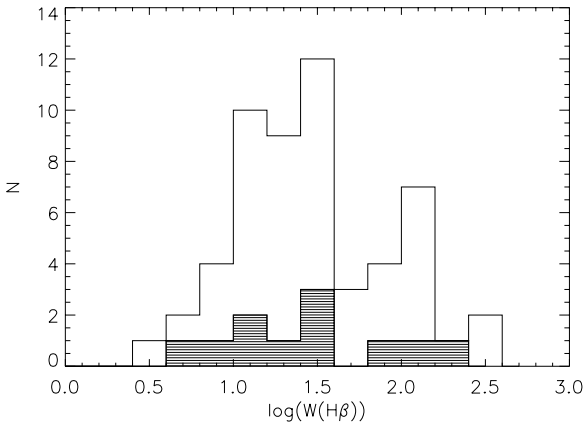

Fig. 2. The distribution of the Hβ equivalent widths (in units of Å). The solid histogram is the distribution of the whole sample, while the hashed histogram is for Void galaxies.

redshifts (Column 3), and the measured equivalent widths of Hβ (Column 4).

All ELGs included in this study were Blue Compact galaxies, and most of them were also dwarfs. The very luminous Starburst Nucleus Galaxies (SBN) were not considered in this sample, the same being true for galaxies with an active nucleus. The BCGs were further classified (Vennik et al. 1999) into the morphological classes proposed by Salzer et al. (1989a,b), namely Dwarf Amorphous Nuclear Starburst Galaxies (DANS), HII Hotspot Galaxies (HIIH), Dwarf HII Hotspot Galaxies (DHIIH), Sargent-Searle Objects (SS), and Interacting Pairs (IP). The classification was done based only on the photometric parameters (absolute magnitude, diameters) and the morphological appearance on the CCD images, as described by Vennik et al. (1999). Nevertheless, an independent check was done using the line ratios of the emission-lines and their location in the diagnostic diagrams, and there is an overall good agreement between the morphological and spectroscopic classification. The type of each galaxy is given in Table 1, Column (10), while their distribution is plotted in Fig. 1.

The distribution of morphological types for Void galaxies is also plotted with hashed-histogram, indicating that galaxies in Voids are spread over all the BCG subtypes. Thus the two samples of Field and Void galaxies consist of the same morphological types; accordingly any differences between the BCGs in these two samples is not due to a different mixture of classes.

3. Star formation properties

We first present the histogram of the Hβ equivalent widths (Fig. 2), which are considered to measure the strength and the age of the star-burst. Large values of the W(Hβ), which means stronger and more recent star-burst are common in both the Field and the Void sample. The same is valid for the low values of the W(Hβ).

Further we use the luminosity of Hβ to estimate the global current star formation rates of the ELGs (Kennicutt 1983). For all the galaxies included in this study the fluxes were measured with a 4″ slit width. For the small projected sizes of our dwarf galaxies, such an aperture is large enough to encompass most of their line emission. Thus we can expect that the Hβ fluxes represent an accurate measurement of the total integrated Hβ fluxes of the galaxies.

For all the galaxies with a strong underlying continuum emission (relative to the Hβ line emission, W(Hβ) < 20 Å) we corrected the Hβ fluxes for underlying stellar absorption with an assumed constant equivalent width of 2 Å (McCall et al. 1985). The Hβ fluxes were corrected for reddening due to dust in our Galaxy and on the galaxy being observed. We used the reddening coefficient c(Hβ), derived from the observed Hα/Hβ Balmer line ratios. For the extinction in our Galaxy we used the standard Galactic reddening law (Whitford 1958) and the extinction values from Burstein & Heiles (1984). Afterwards we corrected for internal extinction making the reasonable assumption that the intrinsic Balmer-line ratios are equal to the case B recombination values of Brocklehurst (1971), for an electron temperature of 10^4 K and an electron density of 100 cm^{-3}. We used the LMC reddening law (Howarth 1983), reckoning that it should be closer to the average reddening law for the dwarf galaxies of our sample than the standard galactic one. The absorption coefficient c(Hβ) is listed for each galaxy in Table 1, Column 5. The Hβ luminosities are computed using a Hubble constant H0 $= 75$ km/s/Mpc and are listed in Table 1, Column 6. In Fig. 3 we give the distribution of the absorption coefficient c(Hβ) for the whole sample as well as for the Void galaxies. Galaxies with differing amounts of internal extinction are spread evenly amongst the Field and Void samples.

Fig. 4 shows the Hβ luminosities against the blue absolute magnitude. The open dots represent the Field galaxies while the filled dots the Void galaxies. As expected, there is a good correlation between the two quantities, and this correlation is present for both Field and Void galaxies. Our Void galaxies seem to occupy the same locus in the diagram as the Field objects, except for the fact that the upper part of the correlation (large blue and Hβ luminosities) is not populated by the Void galaxies.

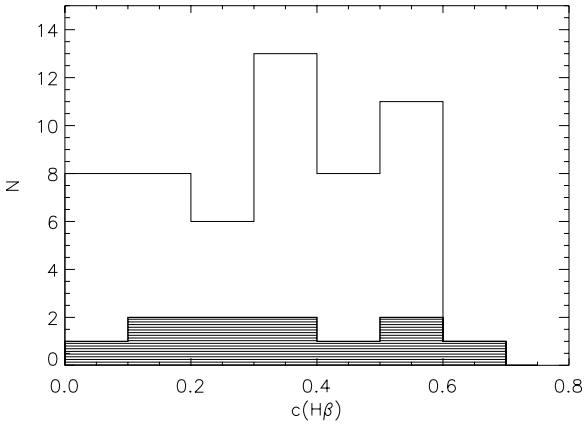

Fig. 3. The distribution of the extinction coefficient c(Hβ). The solid histogram is the distribution of the whole sample, while the hashed histogram is for Void galaxies.

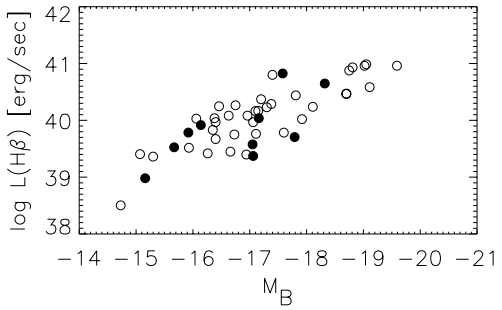

Fig. 4. Logarithm of Hβ luminosity as a function of blue absolute magnitude. Open circles are Field galaxies and filled circles are Void galaxies.

This is once again corroborating evidence (see Popescu et al. 1997) that all our Void galaxies were dwarfs.

The Hβ fluxes were then converted to total SFRs using the calibration of Kennicutt (1998, see also Kennicutt et al. 1994), namely

$$\mathrm{SFR}(\mathrm{M}_\odot\,\mathrm{yr}^{-1}) = \frac{2.85 \times \mathrm{L(H}\beta)}{1.26 \times 10^{41}\mathrm{erg\,s}^{-1}}, \quad (1)$$

again in the case B recombination value of the intrinsic Hα/Hβ Balmer ratio.

The IMF used in this conversion is a Salpeter function dN(m)/dm =-2.35 over the mass range $\mathrm{m} = 0.1$–$100\,\mathrm{M}_\odot$. Kennicutt (1998) indicated that the extended Miller-Scalo IMF used in the calibration of Kennicutt (1983) would produce nearly identical SFRs (only 8% lower). The total SFRs are listed in Table 1, Column 7. The values of the L(Hβ) range between $3.19 \times 10^{38} \leq \mathrm{L(H}\beta) \leq 9.69 \times 10^{40}$ erg/sec, which is equivalent with a range in star formation rates between 0.0072 $\mathrm{M}_\odot$/yr and 2.19 $\mathrm{M}_\odot$/yr.

Despite the fact that there is a clear correlation between M_B and the Hβ luminosity (Fig. 4), L(Hβ) at any given M_B has a scatter of about one order of magnitude. If the total blue magnitude is a good measure of the average past star formation, then the scatter indicates an intrinsic variation in the ratio between the present star formation rate and the average past.

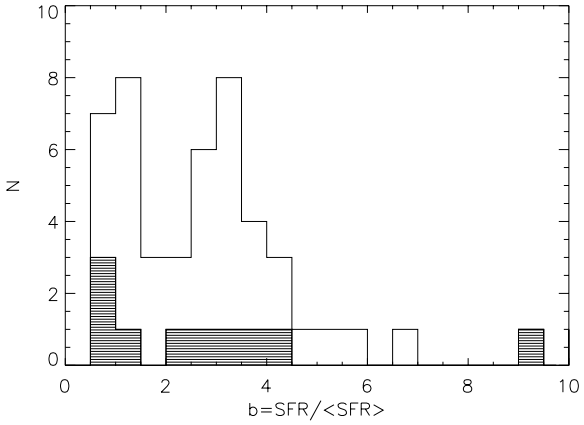

Fig. 5. The distribution of the b ratio between the current SFR and the averaged past SFR. The solid histogram is the distribution of the whole sample, while the hashed histogram is for Void galaxies.

Following again Kennicutt (1983) we derive the ratio of the current SFR to the average past SFR, $\mathrm{b} = \mathrm{SFR}/ < \mathrm{SFR} >$, the latter being derived as the mass of an underlying older disk population, M_d, divided to its age, fixed to 10 Gyr. The disk mass was obtained by multiplying the blue luminosity of the galaxy with an average mass-to-luminosity ratio of 1 $\mathrm{M}_\odot/\mathrm{L}_{B\odot}$. The M/L$_B$ was taken from Kennicutt, Tamblyn & Congdon (1994) (see their Table 3 for the irregular class of galaxies) and it is adopted as an average value for the whole sample of BCDs. Nevertheless, some of the galaxies with strong stellar bursts (larger W(Hβ) values) may have significantly lower mass-to-luminosity ratios, and thus a larger value for the b Scalo parameter. Therefore our b values are only lower limits. While the absolute calibration of the b parameter may be subject of considerable uncertainties (up to a factor of 2), this should not affect the comparison between the b distribution of the Field and Void samples. The result of the calculations (Fig. 5) shows that most of the galaxies are dominated by recent star formation episodes, and there is no trend with the environment. The galaxy with the highest current star-formation rate with respect to the averaged past (a factor 9) is in fact a Void galaxy, HS1507+3743.

Finally, the mean SFR surface density Σ_{SFR} ($\mathrm{M}_\odot\,\mathrm{yr}^{-1}\,\mathrm{kpc}^{-2}$) was derived for each galaxy by dividing the total SFR from Eq. (1) by the area within the isophotal r_{25} radius (in kpc) (Vennik et al. 1999). The derived Σ_{SFR} are listed in Table 1, Column 8 and their distributions are shown in Fig. 6. The histogram of Void galaxies follows that of the Field galaxies.

4. Diagnostic diagrams and metallicities

It has been suggested (Vílchez 1995) that galaxies showing HII region spectra of very high excitation and evidence for hard ionizing spectra, as indicated by the ratio of the [OIII] λ5007,4959/[OII] λ3727, are associated with the low density regions. In Fig. 7 we show that the distribution of the

Table 1.

(1) Galaxy	(2) M_B	(3) z	(4) W(Hβ) [Å]	(5) c(Hβ)	(6) L(Hβ) [erg/sec]	(7) SFR [$M_\odot\,yr^{-1}$]	(8) log Σ_{SFR} [$M_\odot\,yr^{-1}\,kpc^{-2}$]	(9)	(10) type
HS1232+3947	-17.16	0.0210	29	0.286	1.09e+40	0.25	-1.87	V	DHIIH
HS1236+3821	-17.06	0.0073	4	0.602	2.36e+39	0.05	-2.66	V	DHIIH
HS1236+3937	-15.67	0.0184	112	0.081	3.35e+39	0.08	-2.03	V	DHIIH/SS
HS1256+3505	-18.75	0.0342	20	0.448	7.54e+40	0.71	-1.61	F	DANS
HS1258+3438	-16.4	0.0248	36	0.380	9.31e+39	0.21	*	F	DHIIH
HS1301+3325	-16.96	0.0246	11	0.573	1.21e+40	0.27	-1.74	F	DHIIH
HS1301+3209	-17.06	0.0238	10	0.579	9.29e+39	0.21	-1.94	F	HIIH
HS1304+3529	-17.3	0.0165	118	0.013	1.94e+40	0.44	-1.72	F	IP
HS1306+3320	-18.32	0.0270	36	0.508	4.45e+40	1.01	-1.87	V	HIIH
HS1308+3044	-17.92	0.0209	4	0.564	1.05e+40	0.24	-2.13	F	DANS
HS1311+3628	-16.84	0.0031	301	0.160	*	*	*	F	DHIIH
HS1312+3508	-16.26	0.0035	254	0.164	2.62e+39	0.06	-2.33	F	DHIIH
HS1315+3132	-16.46	0.0315	36	0.476	1.77e+40	0.40	-1.45	F	DHIIH
HS1319+3224	-15.3	0.0182	49	0.208	*	*	*	F	SS/DHIIH
HS1325+3255	-15.92	0.0263	74	0.146	6.09e+39	0.14	-1.71	V	DHIIH/SS
HS1328+3424	-17.79	0.0227	8	0.503	5.07e+39	0.11	-2.60	V	HIIH
HS1330+3651	-17.15	0.0167	72	0.147	1.47e+40	0.33	-1.84	F	DHIIH
HS1332+3426	-16.14	0.0220	35	0.444	8.25e+39	0.19	-1.74	V	DHIIH
HS1334+3957	-15.32	0.0083	71	0.000	*	*	*	F	DHIIH
HS1336+3114	-17.94	0.0158	5	0.000	*	*	*	F	HIIH
HS1340+3307	-16.63	0.0158	20	0.539	1.21e+40	0.27	-1.50	F	DHIIH
HS1341+3409	-16.35	0.0171	15	0.480	6.77e+39	0.15	-1.77	F	DHIIH
HS1347+3811	-15.30	0.0103	64	0.243	2.30e+39	0.05	-2.01	F	DHIIH
HS1349+3942	-15.16	0.0054	13	0.337	9.56e+38	0.02	-2.16	V	DHIIH
HS1354+3634	-17.10	0.0167	19	0.513	1.46e+40	0.33	-1.74	F	DANS
HS1354+3635	-17.81	0.0171	21	0.507	2.75e+40	0.62	-1.57	F	HIIH
HS1402+3650	-18.81	0.0347	26	0.561	8.56e+40	1.94	-1.69	F	HIIH
HS1410+3627	-18.11	0.0338	15	0.311	1.73e+40	0.39	-2.11	F	HIIH
HS1416+3554	-16.94	0.0103	14	0.328	2.50e+39	0.06	-2.61	F	DHIIH/HIIH
HS1420+3437	-16.75	0.0246	27	0.448	1.84e+40	0.42	-1.39	F	DHIIH
HS1422+3325	-17.30	0.0341	20	0.337	1.70e+40	0.39	-1.71	F	HIIH
HS1422+3339	-16.4	0.0114	17	0.350	4.68e+39	0.11	*	F	DHIIH/HIIH
HS1424+3836	-16.06	0.0218	104	0.195	1.07e+40	0.24	-1.47	F	DHIIH
HS1425+3835	-17.80	0.0223	12	0.099	*	*	*	F	HIIH
HS1429+4511	-17.40	0.0321	15	0.307	*	*	*	V	DANS
HS1429+3154	-16.73	0.0117	34	0.143	5.63e+39	0.13	-2.04	F	DHIIH
HS1440+4302	-15.07	0.0085	44	0.336	2.54e+39	0.06	-1.82	F	DHIIH/SS
HS1440+3120	-17.4	0.0525	152	0.221	6.32e+40	1.43	*	F	DHIIH
HS1440+3805	-18.80	0.0322	7	0.263	*	*	*	F	HIIH
HS1442+4250	-14.73	0.0025	113	0.081	3.19e+38	0.01	-2.64	F	SS
HS1444+3114	-19.02	0.0297	26	0.413	9.12e+40	2.06	-1.68	F	DANS
HS1502+4152	-16.66	0.0164	7	0.515	2.81e+39	0.06	-2.52	F	DHIIH
HS1507+3743	-17.58	0.0322	232	0.114	6.68e+40	1.51	-1.21	V	DHIIH
HS1529+4512	-17.05	0.0231	16	0.222	3.77e+39	0.09	-2.46	V	HIIH/DHIIH
HS1544+4736	-17.11	0.0195	32	0.025	5.79e+39	0.13	-1.98	F	DHIIH
HS1609+4827	-17.6	0.0096	12	0.381	6.08e+39	0.14	*	F	HIIH
HS1610+4539	-17.2	0.0196	26	0.480	2.35e+40	0.53	*	F	DHIIH/HIIH
HS1614+4709	-13.6	0.0026	140	0.100	8.09e+38	0.02	*	F	SS
HS1633+4703	-15.93	0.0086	15	0.364	3.29e+39	0.07	-1.98	F	DHIIH
HS1640+5136	-19.59	0.0308	21	0.443	9.15e+40	2.07	-1.71	F	SBN/HIIH
HS1641+5053	-19.05	0.0292	15	0.574	9.69e+40	2.19	-1.67	F	HIIH
HS1645+5155	-19.11	0.0286	47	0.330	3.84e+40	0.87	-2.21	F	HIIH
HS1723+5631a	-18.70	0.0286	23	0.341	2.91e+40	0.66	-1.88	F	IP
HS1723+5631b	-18.70	0.0286	32	0.337	2.96e+40	0.67	-1.88	F	IP
HS1728+5655	-16.38	0.0160	106	0.094	1.09e+40	0.25	-1.46	F	DHIIH

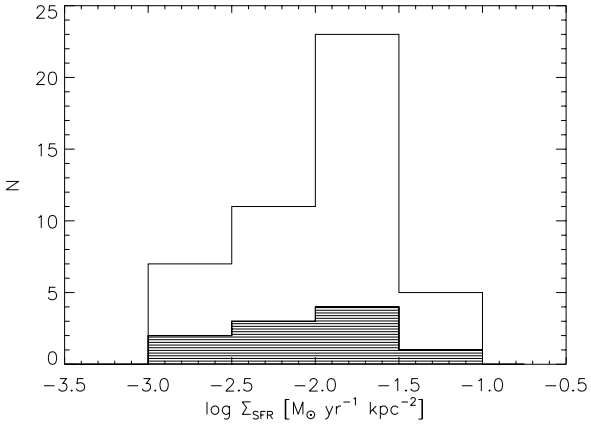

Fig. 6. The distribution of the mean SFR surface density Σ_{SFR}. The solid histogram is the distribution of the whole sample, while the hashed histogram is for Void galaxies.

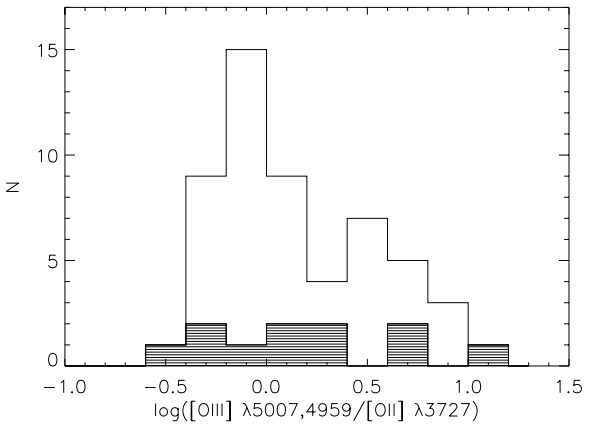

Fig. 7. The distribution of the log([OIII] λ5007,4959/ [OII] λ3727) ratio. The solid histogram is the distribution of the whole sample, while the hashed histogram is for Void galaxies.

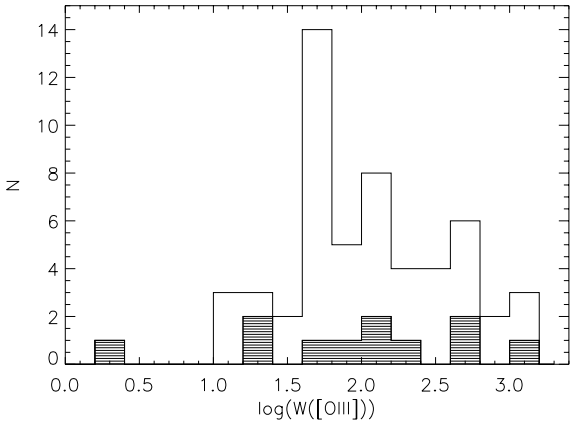

Fig. 8. The distribution of the [OIII] λ5007 equivalent widths (in units of Å). The solid histogram is the distribution of the whole sample, while the hashed histogram is for Void galaxies.

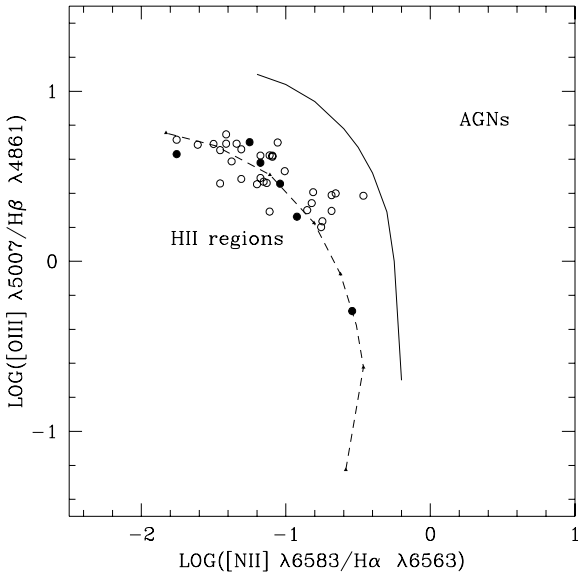

Fig. 9. Line diagnostic of log([OIII] λ5007/Hβ) vs log([NII λ6583/Hα). Open circles are Field galaxies and filled circles are Void galaxies. The dotted curve represents the HII region models of Dopita & Evans (1986), calibrated in metallicity according to Salzer et al. (1989b). The solid triangles located along the curve indicate different values for the metallicity of the gas: 2.0 Z$\odot$ at the lower right-hand end of the curve, with successive symbols representing 1.5, 1.0, 0.75, 0.50, and 0.25 times solar, respectively. The solid line divides AGNs from HII region-like objects.

[OIII]/[OII] is not different between Field and Void galaxies, the same being true for the distribution of the equivalent widths of the [OIII]λ5007 (Fig. 8).

Because accurate measurements of the electron temperature are not available for most of our galaxies, we used diagnostic diagrams (Veilleux & Osterbrock 1987) and the models of Dopita & Evans (1986) in order to obtain oxygen abundances. In Figs. 9 and 10 we plotted the diagnostic diagrams [OIII]/Hβ versus [NII] λ6583/Hα and [OIII]/Hβ versus [OII] λ3727/[OIII] λ5007. Our data seem to follow quite well the models of Dopita & Evans (1986) (shown as dotted lines in the diagnostic diagrams), suggesting that our objects are typical HII galaxies, most of them of high to intermediate excitation, and thus of low to intermediate metallicities. Following Salzer et al. (1989b) we have calibrated the HII model from the diagnostic diagrams in metallicity: from upper left to lower right, 0.25, 0.50, 0.75, 1.0, 1.5 and 2.0 times solar metal abundance (we consider a solar metal abundance 12+log(O/H) = 8.73)). We obtained the metallicity of each object separately, from each diagnostic diagram, and the assigned metallicity was given as an averaged of the two independent estimates. The differences between the two methods are smaller than Δ (12+log(O/H)) = 0.1 dex. We should mention that the zero point of this calibration is not known, but since we are interested only in a relative comparison between Field and Void galaxies, the knowledge of the absolute metallicity is not required.

For a few galaxies the temperature sensitive line [OIII] λ4363 was detected. Our spectra are of low spectral resolution and therefore even for high temperature HII regions it is difficult to obtain an accurate flux value for this line in the

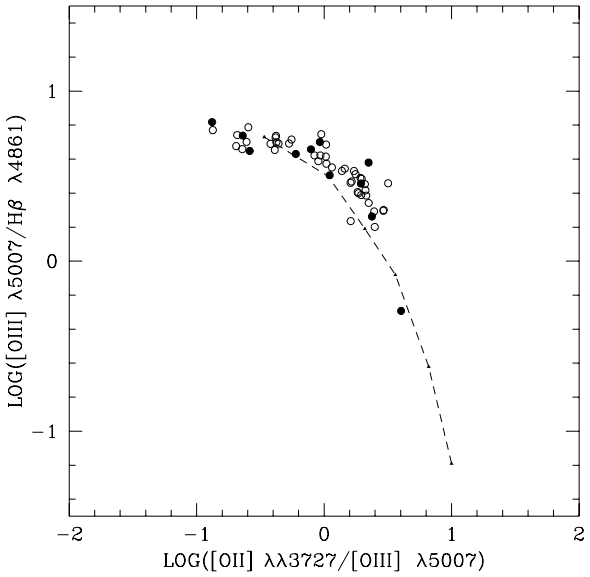

Fig. 10. Line diagnostic of log([OIII] λ5007/Hβ) vs log([OII] λ3727/[OIII] λ5007). Open circles are Field galaxies and filled circles are Void galaxies. The symbols like in Fig. 9.

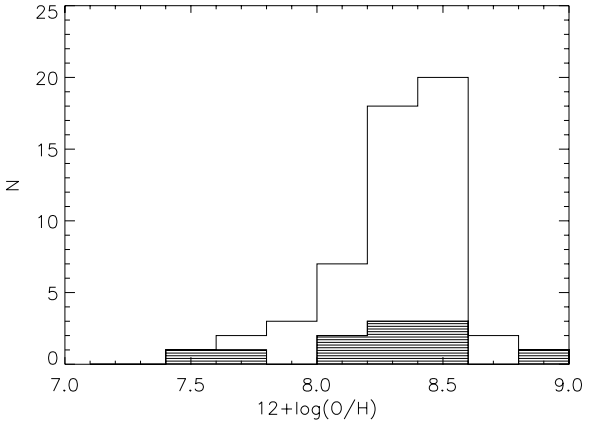

Fig. 11. The distribution of the oxygen abundances 12+log(O/H). The solid histogram is the distribution for the whole sample, while the hashed histogram is for Void galaxies.

blend with the much stronger Hγ line. We used a five level atom program and the ionization correction method of Mathis & Rosa (1991) to obtain O/H abundances. All of these are lower than 0.25 solar, a region where the strong line methods, i.e. of [OIII]/[OII] do not yield O/H unambiguously and/or are rather insensitive to the actual value of O/H. In conclusion we can use the O/H determinations only as an indication of the magnitude of the metallicities, indicated by binning in 0.5 dex intervals in Fig. 11. Nevertheless, Fig. 11 shows again that both the Field and the Void population occupy the same parameter space in metallicity range.

5. The field - cluster dichotomy?

Our study has shown that the dwarf Void galaxies are very similar in their star formation histories and metallicities to Field galaxies of the same morphological type. It appears as if the Void galaxies are unaware of the fact that they exist in huge underdense regions. Going to the opposite environment, we would like to know whether the BCDs in the core regions of rich clusters may show different properties. Our data do not cover any rich cluster, therefore we cannot directly address this question, but we investigated available samples in the literature.

Vílchez (1995) studied the star-forming galaxies in the core of the Virgo Cluster with respect to star-forming galaxies from low density environments. He found a clear trend, with ELGs from low-density environments presenting higher excitation and ionization parameters, higher Hβ equivalent widths, and larger total Hβ luminosities than objects located in the Virgo Cluster core. He interprets these results as being consistent with the existence of two populations of dwarfs, with different origins and evolutionary histories: The BCDs from low density environments experience their first big episodes of star formations, while the Virgo cluster star-forming dwarfs have a mixed star-formation history, requiring continuous star formation in addition to some currently observable bursts.

However, the sample of Virgo cluster core was selected from the Virgo Cluster Catalogue (VCC) of Binggeli et al. (1985), which was based on a visual classification of the direct images, while the dwarfs from low-density regions were taken from the University of Michigan objective-prism survey (MacAlpine & Lewis 1978, MacAlpine & Williams 1981, Salzer 1989). It is well known that objective-prism surveys that use IIIa-J plates are very sensitive in detecting high ionization HII galaxies, since the selection criteria is based on the presence of the [OIII] λ5007 emission line. These kind of surveys can select intrinsically very faint objects, very compact, with almost stellar-like appearance and almost no underlying older stellar population. Such extreme objects can be very easily missed from surveys that select objects based on morphological criteria, or discriminate galaxies from stars based on the apparent diameter of the latter. On the other hand IIIa-J objective prism surveys are less sensitive on lower ionization objects, with stronger Hα lines and stronger continuum, which are better detected from direct plates (or Hα surveys). Therefore we suggest that the dichotomy found by Vílchez between the spectroscopic properties of Virgo Cluster BCDs and star forming galaxies from lower density regions reflect mainly the differences between morphological types, namely between extreme SS/DHIIH galaxies and HIIH/DANS/Im/GI (giant irregular). Vílchez (1995) argued that the BCD and Sm/BCD or Im/BCD classes found in the Virgo core are equivalent with the Salzer HII galaxies.

In order to prove that the BCDs from the Virgo Cluster core are biased towards subtypes of intermediate properties, we have reclassified these objects according to the Salzer classes, based on their morphologies, absolute magnitudes and diameters. We should mention that we did not find any extreme SS type among the Virgo sample. The galaxy VCC1437 from the sample of Vílchez (1995) was not included, since it is considered an Elliptical galaxy in NED. In Fig. 12 we present the distribution of morphological types for the Virgo sample (solid histogram), as compared to the distribution of morphological types for the

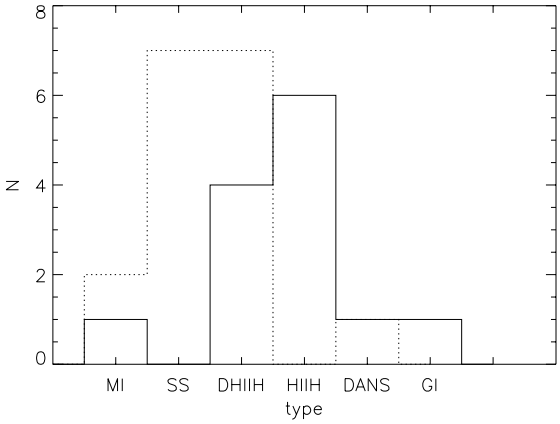

Fig. 12. The distribution of morphological types for the galaxies in the Virgo cluster core (solid histogram) and for the galaxies in the Virgo cluster periphery (dotted histogram).

Virgo cluster periphery. The two distributions are clearly different. The Virgo cluster periphery is dominated by SS and DHIIH galaxies, which consist of very high ionization objects with very recent star bursts, which dominate over the older stellar population. On the other hand the Virgo cluster core is dominated by HIIH galaxies. We conclude that the two samples were not suitable for studying environmental effects since they contain different objects. Nevertheless, it is still possible that the Virgo cluster core is deficient in extreme BCDs of SS/DHIIH type. In order to draw a definitive conclusion one should perform a dedicated search towards the Virgo cluster core, using the same selection criteria as for the Virgo periphery or field regions. We conclude that with the presently available data it is not possible to investigate the influence of the cluster environment on the star-formation properties of BCDs and hence also on their metallicities.

6. Discussion

In the decade following the discovery of BCDs, several investigations based on different samples showed that most of them are metal poor systems (Searle & Sargent 1972, Lequeux et al. 1979, French 1980, Kunth & Sargent 1983). It was thought that some of these galaxies are young systems in the process of forming their first generation of stars. But the detection of an extended faint stellar underlying component in the majority of BCDs (Loose & Thuan 1986, Kunth et al. 1988, Telles et al. (1997), Vennik et al. 1999) supports the idea that they are not truly primordial galaxies, but older LSB dwarf galaxies undergoing transient periods of star formation. A clear demonstration of this two-component structure was recently presented by Schulte-Ladbeck et al. (1998, 1999) for the very nearby BCD VII Zw 403, based on HST photometry of its individual stars down to the red giant branch stars.

Papaderos et al. (1996) proposed a scenario in which the BCDs consist of an old ($\geq$ 10 Gyr) stellar component embedded within a larger self-gravitating gaseous envelope. In this scenario slow infall to the center may produce a central gas density large enough to initiate the first starburst event. A few Myr after the formation of the first massive stellar population, multiple SNe explosions will prevent the cold gas from further collapse. Depending on the mass of the BCD, galactic winds can produce different mass losses of gas and metals. Subsequent infall of the outer HI gas will replenish the cavity in the ISM formed during the previous starburst and, after a quiescent period determined by the gas cooling and mass accretion timescales, the gas density threshold for star formation may be reached again. If we look on the sequence of BCD types, from SS to DANS, we can imagine that smaller LSB will evolve into SS and DHIIH classes, while the bigger ones into HIIH and DANS classes. Since smaller systems have lower gravitational potentials, galactic winds can lead to a significant loss of metals, and thus to the formation of very low metallicity systems.

In the core of rich clusters, the outer gas envelopes of these LSB dwarf may be stripped, leaving the galaxies without their gas reservoir. Then these objects will not have the chance to initiate star-bursts and they will thus not change into BCDs. The smallest systems should be most affected, which may result of a depletion of SS and DHIIH in the core of rich clusters. The results of Vilchez for the star-forming galaxies in the Virgo cluster core can then be explained in these terms. Further, the pressure of the intracluster medium should prevent significant mass loss due to galactic winds, and the surviving BCDs should have higher metallicities than their counterparts in the field. As mentioned in the previous section, until we possess a dedicated, bias free search towards the Virgo cluster core, the discussion above remains very speculative.

In the other extreme environments, the voids, we expect galaxies to have larger gas reservoirs than in field, because here there are no destruction mechanisms. Nevertheless, if the infall of gas is a slow process, producing star bursts in short episodes, then the star-formation properties of these galaxies should not be different from those of field galaxies, as concluded by our study. They may only have enough gas to supply star-bursts for a longer time than in the field, but at the present epoch their properties should not be different.

Recently Lemson & Kauffmann (1999) have considered the environmental influences on dark matter halos and therefore the consequences for the galaxies within them. They use large N-body simulations of dissipationless gravitational clustering in cold dark matter (CDM) cosmologies and they found that the mass of the dark matter halo is the only halo property that correlates significantly with the local environment. The dependence of galaxy morphology, luminosity, surface brightness and star formation rate on environment, must all arise because galaxies are preferentially found in higher mass halos in overdense environments and in lower mass halos in underdense environments. On the other hand, there seem to be little difference between the mass function of dark matter halos for field and void environments. If the models of Lemson and Kauffmann are correct, and indeed there is no correlation between the formation redshifts, concentrations, shapes and spins of the dark matter halos and the overdensity of their local environment, then the star-formation properties of BCDs in Voids and Field are expected

to be similar, at least in the frame of the current hierarchical CDM cosmological models.

In summary, we found that the star formation rates and metallicities of BCDs do not show any significant dependency on environment between the densities encountered in Voids and in the Field. For high-density environments there could be a lack of extreme BCDs of SS/DHIIH type, and therefore a difference in the star-formation properties of cluster BCDs, as suggested by Vílchez (1995) for the Virgo Cluster star-forming galaxies. We argue that available samples in the core of rich clusters are not suitable for this kind of analysis.

Acknowledgements. We would like to thank Dr. Jaan Vennik for performing the morphological classification of the star - forming galaxies in the Virgo Cluster core. We gratefully acknowledge Profs. H. Elsässer and B. Binggeli for interesting discussions. U.H. acknowledges the support of the SFB 375. This research has made use of the NASA/IPAC Extragalactic Database (NED) which is operated by the Jet Propulsion Laboratory, California Institute of Technology, under contract with the National Aeronautics and Space Administration.

References

Binggeli B., Sandage A., Tammann G.A., 1985, AJ 90, 1681
Brocklehurst M., 1971, MNRAS 153, 471
Burstein D., Heiles, C., 1984, ApJS 54, 33
de Lapparent V., Geller M.J., Huchra J.P., 1986, ApJ 302, L1
Dekel A., Silk J., 1986, ApJ 303, 39
Dopita M.A., Evans I.N., 1986, ApJ 307, 431
French H.B., 1980, ApJ 240, 41
Hagen H.-J., Groote D., Engels D., Reimers D., 1995, A&AS 111, 195
Howarth I.D., 1983, MNRAS 203, 301
Huchra J., Geller M., Clemens C., Tokarz S., Michel A., 1992, Bull. C.D.S. 41, 31
Huchra J., Geller M.J., Clemens C.M., Tokarz S.P., Michel A., 1995, The Center for Astrophysics Redshift Catalogue. electronic version
Kennicutt R.C., 1983, ApJ 272, 54
Kennicutt R.C., Tamblyn P., Congdon C.W., 1994, ApJ 435, 22
Kennicutt R.C., 1998, ApJ 498, 541
Kirshner R.P., Oemler A., Schechter P.L., Schectman S.A., 1981, ApJ 248, L57
Kirshner R.P., Oemler A., Schechter P.L., Schectman S.A., 1983a, In: Abell G.O., Chincarini G. (eds.) IAU Symposium 104, Early Evolution of the Universe and Its present Structure. Reidel, Dordrecht, p. 197
Kirshner R.P., Oemler A., Schechter P.L., Schectman S.A., 1983b, AJ 88, 1285
Kunth D., Sargent W.L.W., 1983, ApJ 273, 81
Kunth D., Maurogordato S., Vigroux L., 1988, A&A 204, 10
Lequeux J., Peimbert M., Rayo J.F., Serrano A., Torres-Peimbert S., 1979, A&A 80, 155
Lemson G., Kauffmann G., 1999, MNRAS 302, 111
Loose H.-H., Thuan T.X., 1986, ApJ 309, 59
MacAlpine G.M., Lewis D.W., 1978, ApJS 36, 587
MacAlpine G.M., Williams G.A., 1981, ApJS 45, 113
Mathis J.S., Rosa M.R., 1991, A&A 245, 625
McCall M.L., Rybski P.M., Shields G.A., 1985, ApJS 57, 1
Papaderos P., Loose H.-H., Fricke K.J., Thuan T.X., 1996, A&A 314, 59
Popescu C.C., Hopp U., Hagen H.J., Elsässer H., 1996, A&AS 116, 43
Popescu C.C., Hopp U., Elsässer H., 1997, A&A 328, 756
Popescu C.C., Hopp U., Hagen H.J., Elsässer H., 1998, A&AS 133, 13
Popescu C.C., Hopp U., 1999, in preparation
Ramella, M., Geller M.J., Huchra J.P., 1992, ApJ 384, 396
Rosenberg J.L., Salzer J., Moody J.W., 1994, AJ 108, 1557
Salzer J.J., 1989, ApJ 347, 152
Salzer J.J., MacAlpine G.M., Boroson T.A., 1989a, ApJS 70, 447
Salzer J.J., MacAlpine G.M., Boroson T.A., 1989b, ApJS 70, 479
Sargent W.L.W., Searle L., 1970, ApJ 162, L155
Searle L., Sargent W.L.W., 1972, ApJ 173, 25
Schulte-Ladbeck R.E., Crone M.M., Hopp U., 1998, ApJ 493, L23
Schulte-Ladbeck R.E., Hopp U., Crone M.M., Greggio L., 1999, ApJ in press (astro-ph/9905102)
Szomoru A., van Gorkom J.H., Gregg M.D., 1996, AJ 111, 2141
Telles E., Melnik J., Terlevich R., 1997, MNRAS 288, 78
Veilleux S., Osterbrock D.E., 1987, ApJS 63, 295
Vennik J., Hopp U., Popescu C.C., 1999, in preparation
Vílchez J.M., 1995, AJ 110, 1090
Weistrop D., Hintzen P., Liu C., et al., 1995, AJ 109, 981
Whitford A.E., 1958, AJ 63, 201